# Organic & Biomolecular Chemistry

Accepted Manuscript






ROYAL SOCIETY OF CHEMISTRY

www.rsc.org/obc

Organic Biomolecular Chemistry RSCPublishing

ARTICLE

# Irreversible Covalent Modification of Type I Dehydroquinase by a Stable Schiff Base†

Cite this: DOI: 10.1039/x0xx00000x

Lorena Tizón,[a] María Maneiro,[a] Antonio Peón,[a] José M. Otero,[b] Emilio Lence,[a] Sergio Poza,[a] Mark J. van Raaij,[c] Paul Thompson,[d] Alastair R. Hawkins[d] and Concepción González-Bello*[a]

Received 00th January 2012,
Accepted 00th January 2012

DOI: 10.1039/x0xx00000x

www.rsc.org/

The irreversible inhibition of type I dehydroquinase (DHQ1), the third enzyme of the shikimic acid pathway, has been investigated by structural, biochemical and computational studies. Two epoxides, which are mimetics of the natural substrate, were designed as irreversible inhibitors of the DHQ1 enzyme and to study the binding requirements of the linkage to the enzyme. The epoxide with *S* configuration caused the covalent modification of the protein whereas no reaction was obtained with its epimer. The first crystal structure of DHQ1 from *Salmonella typhi* covalently modified by the *S* epoxide, which is reported at 1.4 Å, revealed that the modified ligand is surprisingly covalently attached to the essential Lys170 by the formation of a stable Schiff base. The experimental and Molecular Dynamics simulation studies reported here highlight the huge importance of the conformation of the C3 carbon of the ligand for covalent linkage to this type of aldolase I enzyme, revealed the key role played by the essential His143 as a Lewis acid in this process and show the need of a neatly closed active site for catalysis.

## Introduction

A promising approach in the search of new antimicrobial or antivirulence agents to combat resistant bacteria[1,2] is a detailed knowledge of the catalytic mechanism and the binding determinants of enzymes involved in biosynthetic pathways or processes that no have mammalian homologues but they are essential for bacterial survival or relevant for virulence. That is the case of the shikimic acid pathway enzymes, through which chorismic acid is biosynthesized. This compound is the precursor in the synthesis of aromatic compounds, including the aromatic amino acids L-Phe, L-Tyr and L-Phe, folate cofactors, ubiquinone and vitamins E and K. Here we report results from structural, biochemical and computational studies conducted to improve our understanding of the irreversible inhibition of dehydroquinase, the third enzyme of the shikimic acid pathway. The dehydroquinase (3-dehydroquinate dehydratase, DHQ, EC 4.2.1.10) is an essential enzyme in relevant pathogenic bacteria such as *Mycobacterium tuberculosis* (*aroD* gene), which is responsible for causing tuberculosis, *Helicobacter pylori* (*aroD/aroQ* gene), the causative agent of gastric and duodenal ulcers, which has also been classified as a type I carcinogen, or *Salmonella enterica subsp. enterica serovar typhimurium* (*aroD* gene), which is one of the pathogens responsible for the majority of human food-borne illness.[3,4] There are two types of DHQ enzymes, namely type I DHQ (DHQ1) and type II DHQ (DHQ2). Both enzymes catalyze the reversible dehydration of 3-dehydroquinic acid (**1**) to form 3-dehydroshikimic acid (**2**) (Scheme 1) but the reaction mechanism is completely different in each case.[5] DHQ1, on which this work focuses, is a class I aldolase enzyme that catalyzes the *syn* elimination of water in **1** by multi-step mechanism that involves the formation of a Schiff base. Nature has found in imine intermediates of this type an excellent way to address a wide range of complex transformations around the chemistry of the carbonyl and the amino groups.[6] A good example is the wide range of reaction types that are catalyzed by PLP-dependent enzymes.[7] The reaction catalyzed by DHQ1 involves the formation of a Schiff base between the carbonyl group of **1** and an essential Lysine (Lys170 in *Salmonella typhi*), the loss of the pro-*R* hydrogen at C2 of **1**, and the acid-catalyzed elimination of the C1 hydroxyl group – a reaction mediated by the essential histidine His143 acting as a proton donor.[5] The crystal structure of the substrate- and product-Schiff bases have been reported.[8] Computational studies also suggested that the product-Schiff base hydrolysis is the rate-determining step.[9-11] By contrast, DHQ2 catalyzes the *anti* elimination of water through the loss of the more acidic pro-*S* hydrogen from C2 of **1** via an enolate intermediate.[12]

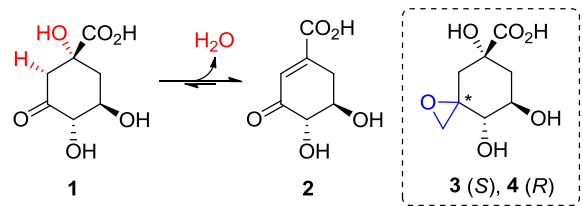


**Scheme 1**. Reaction catalyzed by DHQ1 and target compounds **3**–**4**.

DHQ1 is present in important pathogenic bacteria such as *Salmonella typhi*, *Staphylococcus aureus*, *Escherichia coli* and

*Salmonella enterica subsp. enterica serovar typhimurium.* Moreover, DHQ1 may act as a virulence factor *in vivo* as the deletion of the *aroD* gene, which encodes DHQ1 from *S. typhi* and *Shigella flexneri*, have been proven to afford satisfactory live oral vaccines, with the latter providing monkeys with protection against oral challenge with live *S. flexneri* 2457T.[13-15] Besides these interesting properties, very few irreversible inhibitors[16-17] of DHQ1 have been reported.[18] In addition, although there are available crystal structures of DHQ1 in complex with quinic and shikimic acids,[19-20] both metabolites of the shikimic acid pathway, structural data for DHQ1 covalently modified by these reported irreversible inhibitors have not been reported to date. Such information could give an insight into the irreversible inhibition mechanism and would improve our understanding of this challenging and complex enzyme for the future rational design of inhibitors. To this end, we report here the synthesis of epoxides **3**–**4**, that are mimetics of the natural substrate (Scheme 1). These compounds were designed as irreversible inhibitors of the DHQ1 enzyme and to study the binding requirements of the linkage to the enzyme. The first crystal structure of DHQ1 from *S. typhi* (*St*-DHQ1) covalently modified by epoxide **3** at 1.4 Å is described. Surprisingly, this crystal structure reveals that the epoxide adduct is a Schiff base. Molecular Dynamics (MD) simulation studies were also conducted to obtain further insights into the inhibition mechanism of epoxides **3**–**4** and to understand the experimentally obtained differences between both C3 epimers. These computational studies highlight the importance of the conformation of the C3 carbon of the ligand for covalent linkage to this type of aldolase I enzyme and revealed the key role of the essential His143 in this process.

## Results and discussion

### Synthesis of Compounds 3–4

Compounds **3**–**4** were synthesized *via* epoxidation of an alkene derived from quinic acid. Several alkenes, compounds **5**, were employed to study the diastereselectivity of the reaction (Table 1).

**Table 1** Epoxidation of alkenes **5**

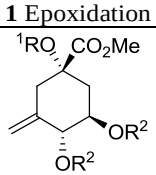


**5**

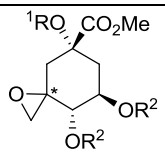


**6** (*R*), **7** (*S*)

| | Substrate | Products, yield (%) | |
|---|---|---|---|
| **5a** | $^1$R = $^2$R = TBS | **6a**, 51[a] | -- |
| **5b** | $^1$R = TMS; $^2$R,$^2$R = acetal[c] | **6b**, 83[b] | -- |
| **5c** | $^1$R = $^2$R = H | -- | **7c**, 65[b] |
| **5d** | $^1$R = H; $^2$R,$^2$R = acetal[c] | **6d**, 32[b] | **7d**, 40[b] |

[a]Reaction conditions: UHP, TFAA, $Na_2HPO_4$, DCM, -78 ºC. [b]Reaction conditions: MCPBA, $NaHCO_3$, DCM, RT. [c]acetal = (*S*,*S*)-C(Me,OMe)-C(Me,OMe)

Full protected alkenes as compounds **5a** and **5b** afforded diastereoselectively the *R*-isomer, compounds **6**, which resulted from the epoxidation from the less hindered face of **5**. By contrast, the presence of the C4 and C1 free hydroxyl groups as compound **5c** favors the epoxidation from the *Si* face due to their orientating effect (see ESI). However, these epoxides **6**–**7** were found to easily undergo nucleophilic ring opening under the basic conditions required to transform these methyl esters into the required acids **3**–**4**. To avoid this problem, methyl ester **5c** was converted into the corresponding benzyl derivative **9** and this group can be easily removed by hydrogenolysis (Scheme 2).

The synthesis of epoxides **3**–**4** was finally achieved from previously described ketone **8**[21,22]. Firstly, methylenation of ketone **8** using Tebbe's reagent gave alkene **5d**, which was then deprotected under acidic conditions to afford triol **5c** in excellent yield. Basic hydrolysis of **5c** followed by alkylation with benzyl bromide gave benzyl ester **9**. Treatment of allylic alcohol **9** with *meta*-chloroperbenzoic acid and sodium bicarbonate gave a chromatographically separable mixture of epoxides **10** and **11** in 57% and 15% yield, respectively. NOE experiments confirmed that the epoxidation is mainly directed by the orientating effect of the allylic hydroxyl group.[21] Irradiation of H8 in epoxide **10** led to enhancement of the signals for Hb (2.7%) and Ha (1.1%). Irradiation of H7 in epoxide **11** led to enhancement of the signal for Hb (1.1%). Finally, catalytic hydrogenolysis of the benzyl esters **10** and **11** gave the desired epoxides **3** and **4**, respectively.

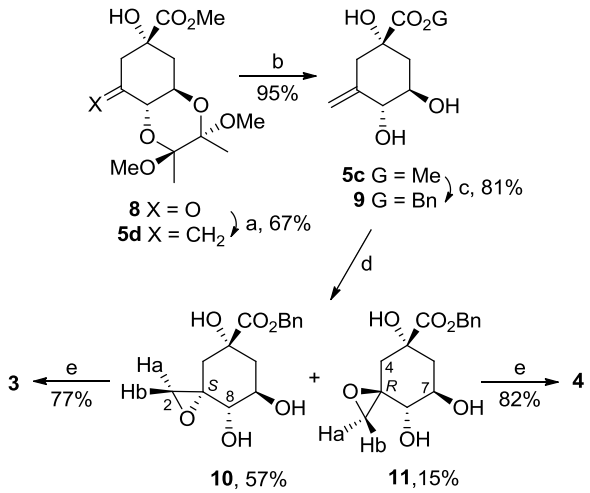


**Scheme 2** Synthesis of epoxides **3**–**4**. *Reagents and conditions*: a, Tebbe's reagent, THF, RT; b, TFA/$H_2O$ (20:1), 0 °C; c, (i) NaOH (aq), THF, RT; (ii) $K_2CO_3$, BnBr, DMF, RT; d, MCPBA, $NaHCO_3$, DCM, RT; e, $H_2$, 10% Pd/C, MeOH, RT.

### Inhibition Activity of Compounds 3–4

The inhibitory properties of compounds **3**–**4** against *St*-DHQ1 were tested. Both epoxides proved to have a highly differentiated activity against *St*-DHQ1. Epoxide **4** proved to be a weak inhibitor with an $IC_{50}$ of 1 mM. A monitoring by $^1$H NMR spectroscopy of a sample of epoxide **4** in the presence of *St*-DHQ1 revealed that no hydrolysis of the epoxide occur after 72 h incubation (Figure S2 of ESI). By contrast, epoxide **3** was found to be a time-dependent irreversible inhibitor of the enzyme (Figure 1). Thus, a 274 µM concentration of epoxide **3** caused ~50% enzyme inactivation in ~30 minutes and after approximately 2 hours 75% inactivation was obtained. Inhibition is also observed at lower concentrations of **3** (110 µM) but it less efficient. Higher concentrations of **3** provide a barely detectable enzymatic activity after approximately 2 hours. It is important to highlight that hydrolysis of the two epoxides was not observed in the absence of enzyme under the assay conditions. In order to obtain further details of the



 

mechanism of action of these inhibitors, structural and MD simulation studies were carried out.

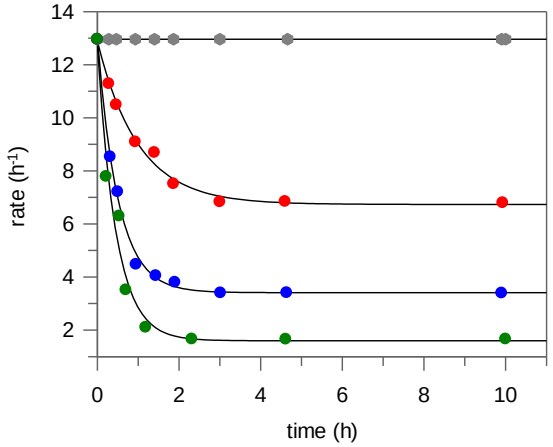


**Figure 1.** Variation of the enzymatic activity of *St*-DHQ1 (1 μM) with time without (•) and after incubation with epoxide **3** [(•) 110 μM, (•) 274 μM and (•) 825 μM]. Results are the average for three observations. Assay conditions were PPB (50 mM, pH 7.2) at 25 °C. The curves were fitted by using the GraFit 5 program (Erithacus Software Ltd.).

### Structural studies

The crystal structure of *St*-DHQ1 covalently modified by its inhibitor **3** was obtained by co-crystallization and it was determined at 1.4 Å. Crystals were cryo-protected with crystallization solution supplemented with 20% glycerol and samples were flash-frozen by rapid immersion in liquid nitrogen. X-ray diffraction data were collected from crystals cryo-cooled in a stream of cold nitrogen gas (100 K) at ambient pressure using synchrotron radiation and the data were subsequently processed. The structure was determined by molecular replacement using the previously described structure of *St*-DHQ1 covalently attached to the active site by Lys170, which was obtained by sodium borohydride reduction of the corresponding product-Schiff base intermediate (PDB entry 1QFE)[5] as a search model, and the structure was refined. A summary of the statistical data following data reduction and processing is given in Table 2.

The resulting *St*-DHQ1/**3** adduct crystallized with two copies in the asymmetric unit (designated as chains A and B) with 0.301 Å rms difference after superposition of $C^{\alpha}$-atom pairs (Figure S3 of ESI). The structure was refined with good geometric parameters and clear electron density is visible for all amino acids with the exception of residues 228–236 in chain A, which are located on the flexible substrate-covering loop and are not visible in this chain. In addition, the ligand cannot be observed in chain A. Comparison of chain B of the crystal structure reported here with that in the previously described structure of the reduced form of the product-Schiff base intermediate (PDB entry 1QFE)[5] shows that both structures are virtually identical (0.262 Å rms difference after superposition of $C^{\alpha}$-atom pairs). In both cases, the flexible loop is in the closed conformation. The closure of this loop forms an additional hydrophobic layer on top of the active site and this is composed of conserved residues Phe145, Met205 and Ala172. MD simulation studies have shown that the sealing of the active site by the entry of the Phe145 side chain inside the site to create a lid is the last step in the formation of the Michaelis complex and it does not occur until the active site is neatly closed by the substrate-covering loop.[24] Met205 seems to be involved in keeping the Phe145 side chain inside the active site by an attractive interaction derived from its location at the edge of the phenyl ring. In this arrangement, the active site is shielded from the solvent environment.

**Table 2**. Crystallographic data collection and refinement statistics for the *St*-DHQ1/**3** adduct[a]

| | |
|---|---|
| *Data processing*[a] | |
| space group | *P*21 |
| cell parameters (a, b, c), Å | a = 60.59, b = 44.47, c = 84.98 (β = 95.2°) |
| wavelength (Å) | 0.87290 |
| detector | Dectris PILATUS 6M |
| observed reflections[b] | 307905 (26338)[c] |
| resolution range (Å) | 47.17 – 1.40 (1.48 – 1.40) |
| Wilson B ($Å^2$) | 9.2 |
| multiplicity | 3.6 (2.7) |
| completeness | 0.960 (0.761) |
| $R_{merge}$ | 0.063 (0.216) |
| *Refinement*[d] | |
| resolution range (Å) | 47.21 – 1.40 (1.48 – 1.40) |
| reflections used in refinement[c] | 81186 (9343) |
| reflections used for $R_{free}$ | 4293 (478) |
| *R* factor[e] | 0.120 (0.152) |
| $R_{free}$[f] | 0.155 (0.214) |
| rmsd (bonds (Å)/angles (°)) | 0.010/1.5 |
| *Final Model* | |
| Protein/inhibitor/water /lithium/chloride atoms | 4009/14/669/1/3 |
| average B protein/inhibitor/ water/lithium/chloride ($Å^2$) | 11.4/17.5/24.0/14.6/28.6 |
| Ramachandran statistics[g] (%) | 99.4/100.0 |
| PDB accession code | 4CLM |

[a]Results from SCALA[31]. [b]No sigma cut-off or other restrictions were used for inclusion of reflections. [c]Values in parentheses are for the highest resolution bin, where applicable. [d]Results from REFMAC[37]. [e]*R*-factor = $\Sigma||Fobs(hkl)| - |Fcalc(hkl)|| / \Sigma|Fobs(hkl)|$. [f]According to Brünger[36]. [g]According to the program MOLPROBITY[38]. The percentages indicated are for residues in favored and total allowed regions, respectively.

Unbiased, calculated electron density maps showed clear electron density for the enzyme-modified inhibitor molecule **3** (Figure 2). The cyclohexane ring of this compound occupies approximately the same site as the cyclohexene ring of the reduced form of the product-Schiff base in PDB entry 1QFE[5] The reported crystal structure shows that the compound is covalently attached to Lys170, which shows two possible arrangements (Figure S4 of ESI), and it binds to the active site by a salt-bridge between its carboxylate group and the guanidinium group of the conserved Arg213, which is the key residue for carboxylate recognition, along with a bidentate hydrogen bond between the carboxylate group of the conserved Glu46 and the C4 and C5 hydroxyl groups of the inhibitor molecule. The latter compound is also anchored in the active site by several additional hydrogen bonds. Thus, the C4 hydroxyl group of the inhibitor interacts by hydrogen bonding with the guanidinium group of the conserved Arg82 and a water molecule (WAT173) that is found in several crystal structures making a bridge between Asp114 and Glu46, probably to avoid

repulsion between the two residues. The C5 hydroxyl group establishes three additional hydrogen bonds, one with the guanidinium group of the conserved Arg48 and two with the side chains of Ser232 and Ser21, both of which are located in the loop that closes the active site. The latter interactions, along with the hydrogen bond between the carboxylate group of the modified inhibitor and the side chain of a conserved Gln236, contribute to close the active site tightly. Moreover, the C1 hydroxyl group of the modified inhibitor and the guanidinium group of Arg82 interact by a bridging water molecule (WAT285). Finally, this structure also revealed key CH-π interactions between the phenyl ring of the conserved Phe225 and the axial hydrogens of the cyclohexane ring of the inhibitor.

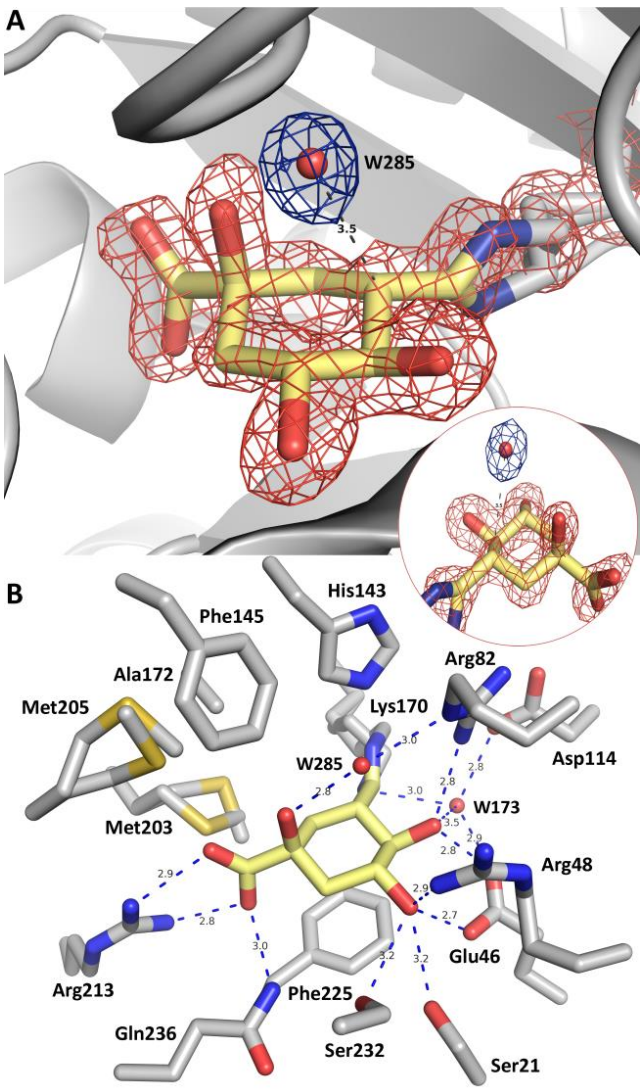


**Figure 2.** Crystal structure of the *St*-DHQ1 covalently modified by epoxide **3**. (A) Unbiased electron density for the modified inhibitor **3** (yellow) and its covalent attachment to Lys170 of *St*-DHQ1 (chain B, gray). From the model obtained by molecular replacement and before inclusion of the inhibitor molecule, refinement was performed to obtain unbiased density for the inhibitor molecule and other model changes. A maximum-likelihood weighted $2F_o - F_c$ map contoured at 1σ is shown up to 1.6 Å around the inhibitor molecule (red) and water molecule W285 (blue). The distance between C3 atom and W285 is shown as dashed lines (black). The final model, including the inhibitor molecule, is superimposed onto the map. (B) Interactions of the modified inhibitor **3** with *St*-DHQ1. Hydrogen bonding and electrostatic interactions (blue) between the ligand and the *St*-DHQ1 are shown. Relevant residues are shown and labeled.

Surprisingly, the crystal structure reported here reveals that the ligand is covalently attached to the enzyme as a Schiff base rather than by the expected hydroxyl amino derivative that would be obtained after nucleophilic ring opening of the epoxide group in **3** by Lys170 as no electron density was observed for the corresponding C3 hydroxyl group (Figure 2A). This finding suggests that additional chemical modifications took place. Also remarkable is the stability against hydrolysis of the experimentally obtained Schiff base. In this context, covalent attachment of DHQ1 from *E. coli* to the product molecule, which is obtained by borohydride reduction of the product-Schiff base, also proved to cause a dramatic increase in the stability of the protein.[25] We believe that this process might also occur with the *St*-DHQ1/**3** adduct and this would explain its stability against hydrolysis. In an effort to gain a further insight into the inhibition mechanism of epoxides **3**–**4** and to understand the experimentally observed differences in inhibitory properties, MD simulation studies were conducted, as it would be discussed below.

### Molecular dynamics simulation studies

The binding modes of compounds **3**–**4** with *St*-DHQ1 were initially studied using GOLD 5.2[26] with the enzyme coordinates found in chain B of the *St*-DHQ1/**3** adduct crystal structure and they were further analyzed by MD simulation studies (10 ns). The corresponding Michaelis complex, *St*-DHQ1/**1**, was also studied. The monomer in aqueous solution using the molecular mechanics force field AMBER[27] was employed. On the basis of results from MD simulations performed with the *St*-DHQ1/**3** adduct and due to mechanistic considerations, a dual protonation of His143 and a deprotonated Lys170 was considered. The binding free energies of compounds **3**–**4** in the active site of *St*-DHQ1 were also calculated using the Molecular Mechanics Poisson–Boltzmann Surface Area (MM/PBSA)[28] approach in explicit water (GB), as implemented in AMBER. These calculations revealed that epoxide **3** has a higher affinity for the enzyme than its epimer **4**, a finding that is consistent with the experimental results (Table S1 of ESI).
It was found that the epoxide **3**, which should bind to the active site as the natural substrate (Figures 3A-3B), remained very stable during the 10 ns of simulation (Figures 3A, S5 and S6). In this binding mode the oxygen atom of the epoxide ring in **3** would be located in close contact with the essential His143 side chain and, to a lesser extent, with the guanidinium group of Arg82 as the natural substrate. Lys170, which is located in the opposite face, is also close to the methylene group of the epoxide moiety in **3**. This can be clearly visualized by analyzing the variation of the distances involving the oxygen atom and the methylene group of the epoxide moiety in **3** and the HE2 atom of His143 and NZ atom of Lys170, respectively, during the whole simulation (Figure 3E). Comparison of the variation of the distances involving the equivalent reactive centers (carbonyl group) of the natural substrate in the Michaelis complex provides a similar situation (Figure 3F).

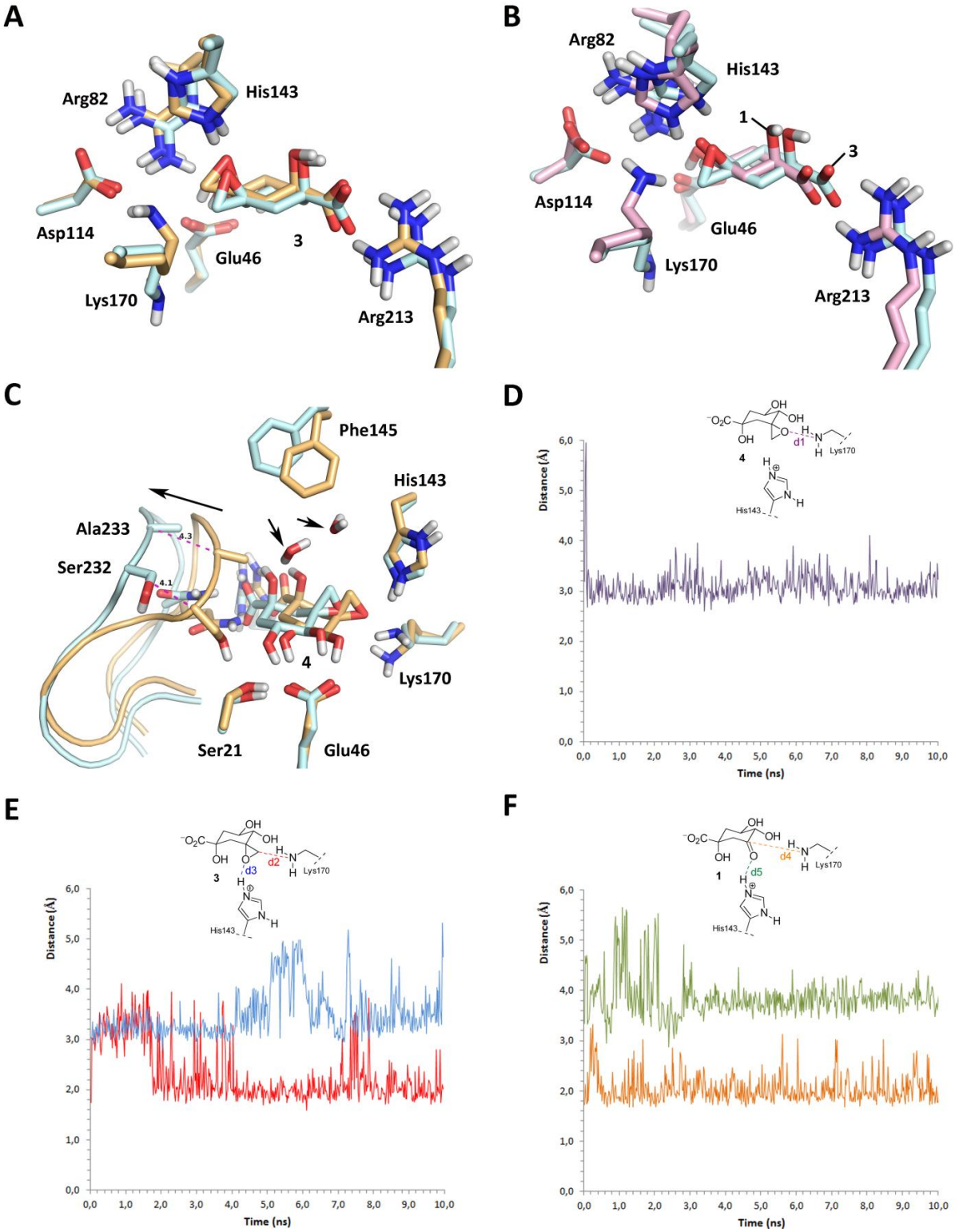


**Figure 3**. Binding mode of epoxides **3**-**4** obtained by MD simulation studies. (A-C) Comparison of results after minimization and prior simulation (orange) and after the dynamic simulation (cyan) with epoxides **3** (A) and **4** (C) in the active site of *St*-DHQ1. Note how epoxide **4** caused the opening of the flexible loop by more than 4 Å (shown as dashed lines in magenta) while no significant changes were observed in the binding mode of epoxide **3**. Relevant side chain residues are shown and labeled. (B) Comparison of the binding mode of the natural substrate (pink) and epoxide **3** (cyan). (D-F) Variation of selected distances in the Michaelis and *St*-DHQ1/**3**-**4** binary complexes during 10 ns simulation: (D) oxygen atom of epoxide **4** and NZ atom of Lys170

(–d1); (E) oxygen atom of epoxide **3** and HE2 atom of His143 (–d3) and methylene group of epoxide ring in **3** and NZ atom of Lys170 (–d2); (F) oxygen atom of carbonyl group in **1** and HE2 atom of His143 (–d5) and carbon atom of carbonyl group in **1** and NZ atom of Lys170 (–d4).

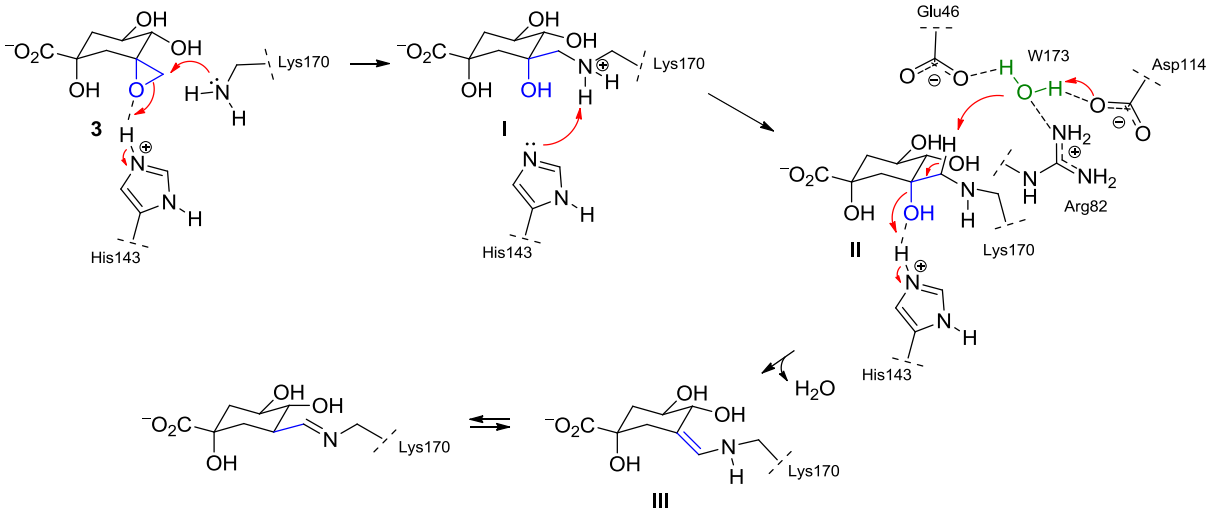


**Scheme 3** Proposed mechanism for the covalent modification of *St*-DHQ1 by **3.**

During the simulation, a significant movement of His143 side chain was observed. Even so, during most of the simulation, the guanidinium group of His143 is closer to the epoxide oxygen than to the carbonyl group of the natural substrate (Figures 3E and 3F). Covalent attachment of **3** would probably occur when the two catalytic residues, His143 and Lys170, are very close to the epoxide moiety. In this arrangement, His143 might act as a Lewis acid by activating and correctly positioning the epoxide group of **3** for nucleophilic attack by the ε-amino group of the essential Lys170 (Scheme 3). The resulting intermediate I could then be deprotonated by the neutral His143 to give the corresponding amino alcohol II. The final steps would be the acid-catalyzed elimination of the tertiary hydroxyl group – a reaction mediated by His143 acting as a proton donor to afford enamine III. Considering the type of residues located in the proximity of the methylene group of II and their disposition, an hydroxide group generated from water molecule W173, which is observed in all the available crystal structures, seems to be the most plausible base for the elimination reaction. W173 has its protons engaged in hydrogen bonding with the carboxylate oxygens of Glu46 and Asp114, and one of its oxygen's lone pairs accepting a hydrogen bond from the guanidinium group of Arg48. On the basis of results from MD simulations performed with the *St*-DHQ1/**3** adduct and the microenvironment around the functional group, Asp114 might be the residue responsible for the deprotonation of W173. The resulted hydroxide group might be stabilized by an electrostatic interaction with the guanidinium group of Arg48. Finally, the resulted enamine III could be in equilibrium with the experimentally observed Schiff base.

In contrast to the above, the MD simulation studies conducted with epoxide **4** showed that this compound, when bound to the active site of *St*-DHQ1, caused the opening of the flexible substrate-covering loop by up to 4.3 Å and a displacement of the His143 side chain from the epoxide moiety (Figure 3C and S5). During the simulation, the amino group of the Lys170 side chain remains in close contact with the oxygen atom of the epoxide ring and with the NE2 group of the His143 side chain (Figure 3D). An extended conformation of the Lys170 side chain is also observed. Significant motions in the position of the Phe145 and Met205 side chains, which are located in the loop that acts as a lid for the active-site cleft, and the entrance of two water molecules in proximity to the epoxide group in **4** were observed. In this arrangement, the active site is not shielded from the solvent environment, which is required for the enzymatic reaction, and no activation of the epoxide ring by His143 might occur. Instead, a strong hydrogen bonding interaction between the ε-amino group of the essential Lys170 and the oxygen atom of the epoxide ring was observed. These findings might explain why epoxide **4** is unable to cause the covalent modification of the enzyme, as experimentally observed.

Therefore, our results suggest that the covalent linkage of these ligands to the enzyme requires the activation by His143 as Lewis acid to allow the nucleophilic attack of Lys170 for the opposite face of the leaving group. Moreover, DHQ1 seems to be specifically designed to perform a nucleophilic attack of Lys170 by the *Si* face of the carbonyl group in **1** after activation by His143 from the opposite face. Moreover, a closed conformation of the substrate-covering loop is also required for the covalent linkage to DHQ1.

## Conclusions and final remarks

The results of the present study show that the epoxide **3** is a good mimetic of the natural substrate because its epoxide moiety has the appropriate stereochemistry to be activated by His143 and it causes the irreversible inhibition of the DHQ1 enzyme by covalent modification. By contrast, its epimer, epoxide **4**, is a weak reversible competitive inhibitor of the enzyme that would cause the opening of the flexible substrate-covering loop. The epoxide moiety of **4** would interact by hydrogen bonding with the ε-amino group of the essential Lys170 that would be in an extended conformation. The crystal structure reported here revealed that the modified ligand **3** is covalently attached to the essential Lys170 by forming a stable



 

Schiff base after several chemical modifications. The results of MD simulation studies suggest that the resulting *St*-DHQ1/**3** adduct is obtained by activation of His143 followed by nucleophilic ring opening of the epoxide and subsequent dehydration and isomerization reactions. To our knowledge, this is the first Schiff base of an aldolase enzyme obtained from an epoxide that has been described.

The structural and computational studies reported provide strong evidence that the enzyme appears to be designed to form the substrate-Schiff base by activation and correct positioning of the oxygen atom of the ketone group in **1** by His143 and subsequent nucleophilic attack by Lys170 from *Si* face of the ketone group. This process requires a shielded active site from the solvent environment by the substrate-covering loop. The results presented here improve our understanding of some of the determinants of irreversible inhibition and provide new insights to be considered in the structure-based design of inhibitors of the DHQ1 enzyme.

## Experimental section

**General information**

All starting materials and reagents were commercially available and were used without further purification. $^1$H NMR spectra (250, 300, 400 and 500 MHz) and $^{13}$C NMR spectra (63, 75, 100 and 125 MHz) were measured in deuterated solvents. *J* values are given in Hertz. NMR assignments were carried out by a combination of 1 D, COSY, and DEPT-135 experiments. FT-IR spectra were recorded as NaCl plates or KBr discs. $[\alpha]_D^{20}$ = values are given in $10^{-1}$ deg cm$^2$ g$^{-1}$. All procedures involving the use of ion-exchange resins were carried out at room temperature using Milli-Q deionized water. Amberlite IR-120 ($H^+$) (cation exchanger) was washed alternately with water, 10% NaOH, water, 10% HCl, and finally water before use.

**Methyl (1*R*,3*S*,4*S*,6*R*,9*R*)-9-hydroxy-3,4-dimethoxy-3,4-dimethyl-7-methylene-2,5-dioxabicyclo[4.4.0]decan-9-carboxylate (5d).** A solution of Tebbe's reagent in toluene (22 mL, 11.07 mmol, *ca.* 0.5 M) was added slowly to a stirred solution of the ketone **8**[21] (3.2 g, 10.06 mmol) in dry THF (50 mL) under argon at 0 ºC. The mixture was stirred at room temperature for 2 h and then was diluted with diethyl ether (125 mL). Aqueous sodium hydroxide (0.1 M, 10–20 drops) was added very slowly and then the mixture was dried ($MgSO_4$), filtered through Celite and evaporated under reduced pressure. The residue was purified by flash column chromatography, eluting with (40:60) ethyl acetate/hexanes, to yield alkene **5d** (2.05 g, 67%) as a colorless oil. $^1$H NMR (300 MHz, $CDCl_3$) δ: 5.29 (q, *J* = 1.8 Hz, 1H, CH*H*), 4.94 (q, *J* = 1.8 Hz, 1H, C*H*H), 4.08 (br d, *J* = 9.0 Hz, 1H, H6), 3.88 (m, 1H, H1), 3.80 (s, 3H, $OCH_3$), 3.26 (s, 3H, $OCH_3$), 3.22 (s, 3H, $OCH_3$), 2.90 (s, 1H, OH), 2.63 (br d, *J* = 13.8 Hz, 1H, $H8_{ax}$), 2.34 (dd, *J* = 13.8 and 3.0 Hz, 1H, $H8_{eq}$), 2.08 (dd, *J* = 12.9 and 12.0 Hz, 1H, $H10_{ax}$), 1.94 (ddd, *J* = 12.9, 4.8 and 3.0 Hz, 1H, $H10_{eq}$), 1.36 (s, 3H, $CH_3$) and 1.30 (s, 3H, $CH_3$) ppm. $^{13}$C NMR (75 MHz, $CDCl_3$) δ: 175.3 (C), 139.0 (C), 109.7 ($CH_2$), 99.7 (C), 99.4 (C), 74.1 (C), 72.3 (CH), 67.9 (CH), 52.9 ($OCH_3$), 47.7 ($OCH_3$), 47.7 ($OCH_3$), 42.8 ($CH_2$), 37.8 ($CH_2$) and 17.6 (2×$CH_3$) ppm.

**Methyl (1*S*,3*R*,4*R*)-1,3,4-trihydroxy-5-methylenecyclohexane-1-carboxylate (5c).** A stirred solution of acetal **5d** (1.0 g, 3.29 mmol) in a (20:1) TFA/$H_2O$ solution (33 mL) was stirred at room temperature for 15 min. The solvent was removed under reduced pressure and the residue resulted was purified by flash chromatography eluting with ethyl acetate to afford compound **5c** (630 mg, 95%) as a colorless oil. $[\alpha]_D^{20}$ = –3° (*c* 1.0, MeOH). $^1$H NMR (250 MHz, $CDCl_3$) δ: 5.25 (s, 1H, C*H*HC), 4.99 (s, 1H, CH*H*C), 3.97 (d, *J* = 8.7 Hz, 1H, H4), 3.81 (s, 3H, $OCH_3$), 3.74 (m, 1H, H3), 2.95 (s, 1H, OH), 2.64 (d, *J* = 13.7 Hz, 1H, $H6_{ax}$), 2.39 (dd, *J* = 13.7 and 2.7 Hz, 1H, $H6_{eq}$), 2.13 (ddd, *J* = 13.0, 5.0 and 3.0 Hz, 1H, $H2_{eq}$) and 1.99 (dd, *J* = 13.0 and 11.2 Hz, 1H, $H2_{ax}$) ppm. $^{13}$C NMR (75 MHz, $CD_3OD$) δ: 176.7 (C), 145.1 (C), 110.8 ($CH_2$), 78.2 (CH), 75.5 (C), 72.7 (CH), 53.0 ($CH_3$), 43.4 ($CH_2$) and 42.0 ($CH_2$) ppm. IR (film) υ: 3400 (OH) and 1730 (CO) cm$^{-1}$. MS (ESI) *m/z* = 225 (M + $Na^+$). HRMS calcd for $C_9H_{14}O_5Na$ (M + $Na^+$): 225.0733; found, 225.0737.

**Benzyl (1*S*,3*R*,4*R*)-1,3,4-trihydroxy-5-methylenecyclohexane-1-carboxylate (9).** A stirred solution of methyl ester **5c** (400 mg, 1.98 mmol) in THF (19.8 mL) was treated with aqueous NaOH (4.0 mL, 1.98 mmol, 0.5 M). After stirring for 30 min, THF was concentrated under reduced pressure and the aqueous solution was diluted with Milli-Q water and ethyl acetate. The organic layer was separated and the aqueous layer was washed with ethyl acetate (×2). The aqueous extract was liophilized to give the corresponding sodium salt (410 mg, 99%) as a colorless oil, which was disolved in dry DMF (19.5 mL) and treated, at room temperature and under argon, with $K_2CO_3$ (810 mg, 5.86 mmol). The resultant solution was treated with benzyl bromide (2.7 mL, 15.62 mmol) and after stirring for 2 h, ethyl acetate and brine were added. The organic layer was separated and the aqueous layer was extracted with ethyl acetate (×5). The combined organic extracts were dried $Na_2SO_4$ (anh.), filtered and concentrated under reduced pressure. The resulted residue was purified by flash chromatography eluting with (50:50) ethyl acetate/hexanes to yield benzyl ester **9** (439 mg, 81%) as a colorless oil. $[\alpha]_D^{20}$ = +10º (*c* 1.8, $CHCl_3$). $^1$H NMR (300 MHz, $CDCl_3$) δ: 7.32 (m, 5H, 5×ArH), 5.21 (s, 1H, C*H*H), 5.19 (d, *J* = 12.3 Hz, 1H, OC*H*H), 5.14 (d, *J* = 12.3 Hz, 1H, OCH*H*), 4.88 (s, 1H, CH*H*), 3.90 (d, *J* = 9.0 Hz, 1H, H4), 3.73 (m, 1H, H3), 2.57 (d, *J* = 14.1 Hz, 1H, $H6_{ax}$), 2.34 (dd, *J* = 14.1 and 2.4 Hz, 1H, $H6_{eq}$), 2.13 (m, 1H, $H2_{eq}$) and 1.95 (dd, *J* = 13.2 and 11.4 Hz, 1H, $H2_{ax}$) ppm. $^{13}$C NMR (75 MHz, $CDCl_3$) δ: 174.8 (C), 142.4 (C), 135.0 (C), 128.6 (2×CH), 128.5 (C), 128.1 (2×CH), 110.6 ($CH_2$), 77.0 (CH), 74.1 (C), 71.9 (CH), 67.7 ($OCH_2$), 42.6 ($CH_2$) and 40.6 ($CH_2$) ppm. IR (film) υ: 3398 (OH) and 1730 (CO) cm$^{-1}$. MS (ESI) *m/z* = 301 (M + $Na^+$). HRMS calcd for $C_{15}H_{18}O_5Na$ (M + $Na^+$): 301.1046; found, 301.1034.

**Epoxidation of alkene 9: benzyl (3*S*,5*R*,7*R*,8*S*)-5,7,8-trihydroxy-1-oxaspiro[2.5]octane-5-carboxylate (10) and benzyl (3*R*,5*R*,7*R*,8*S*)-5,7,8-trihydroxy-1-oxaspiro[2.5]octane-5-carboxylate (11).** A stirred solution of alkene **9** (200 mg, 0.72 mmol) in dry dichloromethane (7.0 mL), at room temperature and under argon, was treated with MCPBA (130 mg, 1.80 mmol) and sodium bicarbonate (90 mg, 1.08 mmol). After stirring for 20 h, potassium carbonate was added and the suspension was filtered. The filtrate and the washings were concentrated under reduced pressure. The resulted residue was purified by flash chromatography eluting with a gradient of ethyl acetate/hexanes [(75:25) to (100:0)] to afford epoxides **10** (120 mg, 57%) and **11** (31 mg, 15%). The stereochemistry of new chiral center of both epoxides was determined by NOE experiments. The stereochemistry of C1 in **10** is supported by the enhancement of the $H_a$ (1.1%) and $H_b$ (2.7%) signals resulted of the inversion of H8 signal. The enhancement of the $H_b$ signal resulted of the inversion of H7 signal (1.1%) supports the C1 stereochemistry of **11**.

**10**: Colorless oil. $[\alpha]_D^{20}$ = –4º (*c* 1.2, MeOH). $^1$H NMR (300 MHz, $CD_3OD$) δ: 7.34 (m, 5H, 5×ArH), 5.20 (d, *J* = 12.3 Hz, 1H, C*H*HPh), 5.15 (d, *J* = 12.3 Hz, 1H, CH*H*Ph), 3.94 (ddd, *J* =

10.8, 9.3 and 4.5 Hz, 1H, H7), 3.59 (d, *J* = 9.3 Hz, 1H, H8), 2.87 (d, *J* = 5.1 Hz, 1H, C*H*HO), 2.48 (d, *J* = 14.7 Hz, 1H, $H4_{ax}$), 2.41 (d, *J* = 5.1 Hz, 1H, CH*H*O), 2.19 (ddd, *J* = 13.5, 4.5 and 3.0 Hz, $H6_{eq}$), 1.92 (dd, *J* = 13.5 and 10.8 Hz, $H6_{ax}$) and 1.59 (dd, *J* = 14.7 and 3.0 Hz, $H4_{eq}$) ppm. $^{13}$C NMR (75 MHz, $CD_3OD$) δ: 174.3 (C), 135.1 (C), 128.6 (2×CH), 128.5 (CH), 128.2 (2×CH), 74.5 (C), 72.6 (CH), 69.3 (CH), 67.6 ($CH_2$), 58.0 (C), 46.3 ($CH_2$), 40.5 ($CH_2$) and 39.6 ($CH_2$) ppm. IR (film) υ: 3417 (OH) and 1732 (CO) cm$^{-1}$. MS (ESI) *m/z* = 317 (M + $Na^+$). HRMS calcd for $C_{15}H_{18}O_6Na$ (M + $Na^+$): 317.0996; found, 317.1001.

**11**: White solid. Mp: 108–111 °C. $[\alpha]_D^{20}$ = +7° (*c* 1.3, $CHCl_3$). $^1$H NMR (300 MHz, $CD_3OD$) δ: 7.33 (m, 5H, 5×ArH), 5.20 (d, *J* = 12.6 Hz, 1H, PhC*H*HO), 5.16 (d, *J* = 12.6 Hz, 1H, PhCH*H*O), 3.80 (m, 1H, H7), 3.59 (d, *J* = 9.3 Hz, 1H, H8), 3.09 (dd, *J* = 5.4 and 1.2 Hz, 1H, C*H*HO($H_b$)), 2.58 (d, *J* = 5.4 Hz, 1H, CH*H*O($H_a$)), 2.38 (dd, *J* = 13.5 and 1.2 Hz, 1H, $H4_{ax}$), 2.13 (ddd, *J* = 13.2, 4.5 and 3.0 Hz, 1H, $H6_{eq}$), 1.88 (dd, *J* = 13.2 and 11.4 Hz, 1H, $H6_{ax}$) and 1.49 (dd, *J* = 13.5 and 3.0 Hz, 1H, $H4_{eq}$) ppm. $^{13}$C NMR (75 MHz, $CD_3OD$) δ: 175.6 (C), 133.8 (C), 129.6 (2×CH), 129.4 (CH), 129.3 (2×CH), 75.2 (C), 75.1 (CH), 71.1 (CH), 68.2 ($OCH_2$), 59.4 (C), 50.6 ($OCH_2$), 41.9 ($CH_2$) and 41.6 ($CH_2$) ppm. IR (KBr) υ: 3421 (OH) and 1733 (CO) cm$^{-1}$. MS (ESI) *m/z* = 317 (M + $Na^+$). HRMS calcd for $C_{15}H_{18}O_6Na$ (M + $Na^+$): 317.0996; found, 317.0984.

**(3*S*,5*R*,7*R*,8*S*)-5,7,8-Trihydroxy-1-oxaspiro[2.5]octane-5-carboxylic acid (3).** A suspension of benzyl ester **10** (40 mg, 0.14 mmol) and Pd/C (4 mg, 5%) in ethyl acetate (30 mL), was stirred at room temperature and under hydrogen atmosphere for 8 h. After removal of the hydrogen atmosphere, the suspension was filtered over a plug of Celite. The filtrate and the washings (ethyl acetate) were concentrated under reduced pressure to afford acid **3** (22 mg, 77%) as a white solid. Mp: 150–153 °C (dec.). $[\alpha]_D^{20}$ = +12° (*c* 2.5, MeOH). $^1$H NMR (300 MHz, $CD_3OD$) δ: 3.94 (ddd, *J* = 11.1, 9.3 and 4.5 Hz 1H, H7), 3.62 (d, *J* = 9.3 Hz, 1H, H8), 2.90 (d, *J* = 5.1 Hz, 1H, C*H*HO ($H_a$)), 2.52 (d, *J* = 14.7 Hz, 1H, $H4_{ax}$), 2.42 (d, *J* = 5.1 Hz, 1H, CH*H*O($H_b$)), 2.17 (ddd, *J* = 13.2, 4.5 and 3.0 Hz, 1H, $H6_{eq}$), 1.92 (dd, *J* = 13.2 and 11.1 Hz, 1H, $H6_{ax}$) and 1.56 (dd, *J* = 14.7 and 3.0 Hz, 1H, $H4_{eq}$) ppm. $^{13}$C NMR (75 MHz, $CD_3OD$) δ: 178.0 (C), 76.5 (C), 73.9 (CH), 70.3 (CH), 59.1 (C), 46.8 ($OCH_2$), 42.1 ($CH_2$) and 40.7 ($CH_2$) ppm. IR (KBr) υ: 3303 (OH) and 1716 (CO) cm$^{-1}$. MS (ESI) *m/z* = 203 (M – H). HRMS calcd for $C_8H_{11}O_6$ (M – H): 203.0561; found, 203.0556.

**(3*R*,5*R*,7*R*,8*S*)-5,7,8-Trihydroxy-1-oxaspiro[2.5]octane-5-carboxylic acid (4).** A suspension of benzyl ester **11** (20 mg, 0.07 mmol) and Pd/C (2 mg, 5%) in ethyl acetate (15 mL), was stirred at room temperature and under hydrogen atmosfere for 8 h. After removal of the hydrogen atmosphere, the suspension was filtered over a plug of Celite. The filtrate and the washings (ethyl acetate) were concentrated under reduced pressure to afford acid **4** (20 mg, 82%) as a white solid. Mp: 128–131 °C (dec.). $[\alpha]_D^{20}$ = –6° (*c* 1.8, MeOH). $^1$H NMR (250 MHz, $CD_3OD$) δ: 3.82 (ddd, *J* = 11.5, 9.2 and 5.0 Hz 1H, H7), 3.62 (d, *J* = 9.2 Hz, 1H, H8), 3.11 (dd, *J* = 5.3 and 1.5 Hz, 1H, C*H*HO), 2.60 (d, *J* = 5.3 Hz, 1H, CH*H*O), 2.41 (dd, *J* = 13.5 and 1.5 Hz, 1H, $H4_{ax}$), 2.12 (ddd, *J* = 13.5, 5.0 and 3.0 Hz, 1H, $H6_{eq}$), 1.90 (dd, *J* = 13.5 and 11.5 Hz, 1H, $H6_{ax}$) and 1.48 (dd, *J* = 13.5 and 3.0 Hz, 1H, $H4_{eq}$) ppm. $^{13}$C NMR (63 MHz, $CD_3OD$) δ: 177.9 (C), 75.3 (CH), 74.8 (C), 71.2 (CH), 59.6 (C), 50.6 ($OCH_2$), 42.0 ($CH_2$) and 41.7 ($CH_2$) ppm. IR (KBr) υ: 3396 (OH) and 1702 (CO) cm$^{-1}$. MS (ESI) *m/z* = 227 (M + $Na^+$). HRMS calcd for $C_8H_{12}O_6Na$ (M + $Na^+$): 227.0526; found, 227.0530.

**Dehydroquinase assays**. The *St*-DHQ1 enzyme was purified as described previously.[29] Concentrated solutions of *St*-DHQ1 (0.85 mg mL$^{-1}$, 30.74 μM) were stored in potassium phosphate buffer (50 mM) and DTT (1 mM) at pH 6.6 at –80 °C. When required for assays, aliquots of the enzyme stocks were diluted into water and buffer and stored on ice. Dehydroquinase was assayed in the forward direction by monitoring the increase in absorbance at 234 nm in the UV spectrum due to the absorbance of the enone-carboxylate chromophore of 3-dehydroshikimic acid (**2**) (ε/M$^{-1}$ cm$^{-1}$ 12 000). Standard assay conditions were PPB (50 mM, pH 7.2) at 25 °C. Each assay was initiated by addition of the substrate. Solutions of 3-dehydroquinic acid (**1**) were calibrated by equilibration with DHQ1 and measurement of the change in the UV absorbance at 234 nm due to the formation of the enone-carboxylate chromophore of 3-dehydroshikimic acid (**2**). Under assay conditions, the kinetic parameters of *St*-DHQ1 were $K_m$ = 24 ± 3 μM and $k_{cat}$ = 1.1 ± 0.1 s$^{-1}$.

**Inhibition assays**. 15 μL of *St*-DHQ1 enzyme stocks (30.7 μM, 0.85 mg mL$^{-1}$) was independently incubated with 4, 10 and 30 μL of aqueous stocks solutions of epoxide **3** (13.7 mM) in 50 mM PPB at pH 7.2 at 25 °C in a total volume of 500 μL. Epoxide **3** inhibition assay concentrations: 110, 274 and 825 μM, respectively. Under the same assay conditions, the activity of the *St*-DHQ1 enzyme was simultaneously followed as a control in the absence of epoxide **3**. The activity was progressively determined over 24 h period under the standard assay conditions (see above) using aliquots (8 μL) from the incubation samples and the control and 50 μL of a 0.27 mM solution of 3-dehydroquinic acid (**1**). The initial rates at the above mentioned fixed enzyme, epoxide **3** and substrate concentrations were measured and plotted against time. The $IC_{50}$ of compound **4** against *St*-DHQ1 was obtained by measuring the initial rates at fixed enzyme and substrate concentrations (~$K_m$) in the absence and in the presence of various inhibitor concentrations.

**Crystallization of *St*-DHQ1/3 adduct.** *St*-DHQ1 was concentrated to 8 mg mL$^{-1}$ in 10 mM Tris.HCl pH 7.4 and 40 mM potassium chloride. Compound **3** was dissolved at 0.25 M in methanol and added at a ratio of 1:20 (v/v) to the protein solution to give a solution of approximately 10 equivalents of **3** per protein monomer. Plate-shaped crystals of up to 0.1 mm × 0.1 mm of the *St*-DHQ1/**3** adduct were obtained after four weeks of vapor diffusion in sitting drops comprised of 2.0 μL protein/inhibitor solution mixed with 2.0 μL reservoir solution against 0.15 mL reservoirs containing 34% (w/v) polyethyleneglycol 4000 and 0.1 M citrate/phosphate pH 5.6.

**Structure determination of *St*-DHQ1/3 adduct.** Crystals were mounted into cryoloops and directly flash frozen by rapid immersion in liquid nitrogen. X-ray diffraction data for *St*-DHQ1/**3** adduct was collected on beamline ID23-2 (ESRF, Grenoble, France) from a crystal maintained at 100 K. The diffraction data were processed, scaled, corrected for absorption effects and the crystal unit-cell parameters calculated by global refinement using XDS,[30] SCALA[31] and other programs within the CCP4 software suite.[32] The structure was solved by molecular replacement, using the program MOLREP[33] with a search model generated from PDB entry 1QFE[5]. Inhibitor´s structure and geometrical restraints were generated with the PRODRG2 server[34] and it was manually placed during the model building, which was performed with COOT.[35] Reflections for calculating Rfree[36] were selected randomly. The



 

refinement of the models was performed with REFMAC[37] and final structure validation was performed with MOLPROBITY.[38] The data collection, refinement and model statistics are summarized in Table 2. Structure figures were prepared using PYMOL.[39]

**Molecular dynamics simulations.** *Ligand minimization*. Ligand geometries were optimized using a restricted Hartree–Fock (RHF) method and a 6–31G(d,p) basis set, as implemented in the *ab initio* program Gaussian 09.[40] The charge distribution for each ligand studied was obtained by fitting the quantum mechanically calculated (B3LYP/cc-pVTZ and IEF-PCM as solvation model) molecular electrostatic potential (MEP) of the geometry-optimized molecule to a point charge model, as implemented in the assisted model building with energy refinement (AMBER)[41] suite of programs. The missing bonded and non-bonded parameters were assigned, by analogy or through interpolation from those already present in the AMBER database (GAFF).[42]

*Generation and minimization of the DHQ1-ligand complexes*. Simulations were carried out using the enzyme geometries found in the crystal structure of *St*-DHQ1/**3** adduct. The monomer (chain B) was used for these studies. For *St*-DHQ1/**3**-**4** binary complexes, the covalently linked ligand was manually replaced by epoxides **3**–**4**, respectively. Crystallographic water molecules were maintained. Hydrogens were added to the protein using the web-based PROPKA3.1 server,[43] which assigned protonation states to all titratable residues at the chosen pH of 7.0. However, δ and/or ε protonation was manually corrected for His143 (dual) of the active site due to mechanistic considerations and on the basis of results from preliminary MD simulations. Molecular mechanics parameters from the ff12SB and GAFF force fields, respectively, were assigned to the protein and the ligands using the LEaP module of AMBER 12.[44] All terminal hydrogens were first minimized in vacuum (2000 steps, half of them steepest descent, the other half conjugate gradient). Energy minimization was carried out in two stages using the implicit solvent GB model; firstly protein side chains (2000 steps, idem) and secondly the entire complex (1000 steps, idem). Thereafter, each molecular system was immersed in a truncated octahedron containing TIP3P[45] water molecules (10 Å radius) and $Na^+$ ions[46] to achieve electroneutrality.

*Simulations.* MD simulations were performed using the AMBER 11.0 suite of programs and Amber ff12SB force field. Periodic boundary conditions were applied and electrostatic interactions were treated using the smooth particle mesh Ewald method (PME)[47] with a grid spacing of 1 Å. The cutoff distance for the non-bonded interactions was 9 Å. The SHAKE algorithm[48] was applied to all bonds containing hydrogen, using a tolerance of $10^{-5}$ Å and an integration step of 2.0 fs. Minimization was carried out in three steps, starting with the octahedron water hydrogens, followed by solvent molecules and sodium counterions and finally the entire system. The minimized system was heated at 300 K (1 atm, 25 ps, a positional restraint force constant of 50 kcal $mol^{-1}$ $Å^{-2}$). These initial harmonic restraints were gradually reduced to 5 kcal $mol^{-1}$ $Å^{-2}$ (10 steps) and the resulting systems were allowed to equilibrate further. MD were carried out for 10 ns. System coordinates were collected every 20 ps for further analysis.

## Acknowledgements

Financial support from the Spanish Ministry of Science and Innovation (SAF2013-42899-R), Xunta de Galicia (GRC2013-041) and the European Regional Development Fund (ERDF) is gratefully acknowledged. LT, AP and MM thank the Spanish Ministry of Education for their respective FPU fellowships. EL and JMO thank and the Xunta de Galicia for their respective postdoctoral fellowships. We thank ESRF, synchrotron beamline ID23-2 (Grenoble, France), for the provision of beam time. We are also grateful to the Centro de Supercomputación de Galicia (CESGA) for use of the Finis Terrae computer.

## Notes and references

[a] Centro Singular de Investigación en Química Biológica y Materiales Moleculares (CIQUS), Universidad de Santiago de Compostela, calle Jenaro de la Fuente s/n, 15782 Santiago de Compostela, Spain.

[b] Departamento de Bioquímica y Biología Molecular and CIQUS, Universidad de Santiago de Compostela, 15782 Santiago de Compostela, Spain.

[c] Departamento de Estructura de Macromoléculas, Centro Nacional de Biotecnología (CSIC), Campus Cantoblanco, 28049 Madrid, Spain.

[d] Institute of Cell and Molecular Biosciences, Medical School, University of Newcastle upon Tyne, Newcastle upon Tyne NE2 4HH, UK.

* E-mail: concepcion.gonzalez.bello@usc.es

† Coordinates and structure factors of the reported crystal structure are available from the Protein Data Bank with accession code 4CLM. X-ray crystal structure of epoxide **6a** is available from the Cambridge Crystallographic Data Centre via www.ccdc.cam.ac.uk/data_request/cif [or from the Cambridge Crystallographic Data Centre, 12 Union Road, Cambridge CB2 1EZ, UK; Fax: (+44)-1223-336033; E-mail: deposit@ccdc.cam.ac.uk] with accession code CCDC 993317.

Electronic Supplementary Information (ESI) available: [experimental procedures for the synthesis and characterization of compounds **5a, 5b**, **6a**, **6b**, **6d**, **7c** and **7d**, X-ray structure of epoxide **6a** (CCDC 993317) and extra figures of the NMR, MD simulation and structural studies are included]. See DOI: 10.1039/b000000x/

1 M. Mckenna, *Nature*, 2013, **499**, 394.
2 M. A. Fischbach, C. T. Walsh, *Science*, 2009, **325**, 1089.
3 Data base for essential genes in bacteria see www.essentialgene.org
4 R. Zhang, and Y. Lin, *Nucleic Acids Res.*, 2009, **37**, D455.
5 D. G. Gourley, A. K. Shrive, I. Polikarpov, T. Krell, J. R. Coggins, A. R. Hawkins, N. W. Isaacs, and L. Sawyer, *Nat. Struct. Biol.*, 1999, **6**, 521.
6 E. Ritter, P. Przybylski, B. Brzezinski, and F. Bartl, *Curr. Org. Chem*. 2009, **13**, 241.
7 (a) A. C. Eliot, and J. F. Kirsch, *Ann. Rev. Biochem*. 2004, **73**, 383. (b) A. Amadasi, M. Bertoldi, R. Contestabile, S. Bettati, B. Cellini, M. L. di Salvo, C. Borri-Voltattorni, F. Bossa, and A. Mozzarelli, *Curr. Med. Chem*. 2007, **14**, 1291.
8 S. H. Light, G. Minasov, L. Shuvalova, M. E. Duban, M. Caffrey, W. F. Anderson, and A. Lavie, *J. Biol. Chem.*, 2011, **286**, 3531.
9 Y. Yao, and Z.-S. Li, *Org. Biomol. Chem.*, 2012, **10**, 7037.
10 Y. Yao, and Z.-S. Li, *Chem. Phys. Lett.*, 2012, **519**-**520**, 100.
11 Q. Pan, Y. Yao, and Z.-S. Li, *Theor. Chem. Acc.*, 2012, **131**, 1204.
12 C. Cloderch, E. Lence, A. Peón, H. Lamb, A. R. Hawkins, F. Gago, and C. González-Bello, *Biochem. J.*, 2014, **458**, 547.
13 (a) C. O. Tacket, D. M. Hone, R. Curtiss III, S. M. Kelly, G. Losonsky, L. Guers, A. M. Harris, R. Edelman, and M. M. Levine, *Infection and Immunity*, 1992, **60**, 536. (b) A. Karnell, P. D. Cam, N. Verma, and A. A. Lindberg, *Vaccine*, 1993, **11**, 830.

14 C. O. Tacket, D. M. Hone, G. Losonsky, L. Guers, R. Edelman, and M. M. Levine, *Vaccine*, 1992, **10**, 443.
15 R. Racz, M. Chung, Z. Xiang and Y. He, *Vaccine*, 2013, **31**, 797.
16 T. D. H. Bugg, C. Abell, and J. R. Coggins, *Tetrahedron Lett.*, 1998, **29**, 6783.
17 C. González-Bello, J. M. Harris, M. K. Manthey, J. R. Coggins, and C. Abell, *Bioorg. Med. Chem. Lett.*, 2000, **10**, 407.
18 For no covalent DHQ1 inhibitors see: K. Ratia, S. H. Light, A. Antanasijevic, W. F. Anderson, M. Caffrey, and A. Lavie, *PLoS ONE*, 2014, **9**, e89356.
19 S. H. Light, A. Antanasijcvic, S. N. Krishna, M. Caffrey, W. F. Anderson, and A. Lavie, *Biochemistry*, 2014, **53**, 872.
20 S. H. Light, G. Minasov, L. Shuvalova, S. N. Peterson, M. Caffrey, W. F. Anderson, and A. Lavie, *Biochemistry* **2011**, *50*, 2357.
21 M. D. Toscano, M. Frederickson, D. P. Evans, J. R. Coggins, C. Abell, and C. González-Bello, *Org. Biomol. Chem.*, 2003, **1**, 2075.
22 F. Tian, J.-L. Montchamp, and J. W. Frost, *J. Org. Chem.*, 1996, **61**, 7373.
23 H. C. Kolb, M. S. VanNieuwenhze, and K. B. Sharpless, *Chem. Rev.*, 1994, **94**, 2483.
24 M. Maneiro, A. Peón, E. Lence, J. M. Otero, M. J. van Raaij, P. Thompson, A. R. Hawkins, and C. González-Bello, *Biochem. J.*, 2014, **462**, 415.
25 A. Reilly, P. Morgan, K. Davis, S. M. Kelly, J. Greene, A. J. Rowe, S. E. Harding, N. C. Price, J. R. Coggins, and C. Kleanthous, *J. Biol. Chem.*, 1994, **269**, 5523.
26 http://www.ccdc.cam.ac.uk/products/life_sciencies/gold/
27 W. D. Cornell, P. Cieplak, C. I. Bayly, I. R. Gould, K. M. Merz, D. M. Ferguson, D. C. Spellmeyer, T. Fox, J. W. Caldwell, and P. A. Kollman, *J. Am. Chem. Soc.*, 1995, **117**, 5179.
28 B. R. Miller III, T. D. McGee Jr., J. M. Swails, N. Homeyer, H. Gohlke, and A. E. Roitberg, *J. Chem. Theory Comput.*, 2012, **8**, 3314.
29 J. D. Moore, A. R. Hawkins, I. G. Charles, R. Deka, J. R. Coggins, A. Cooper, S. M. Kelly, and N. C. Price, *Biochem. J.*, 1993, **295**, 277.
30 W. Kabsch, *Acta Cryst.*, 2010, **D66**, 125.
31 P. Evans, *Acta Cryst.*, 2006, **D62**, 72.
32 M. D. Winn, *J. Synchrotron Radiat.*, 2003, **10**, 23.
33 A. Vagin, and A. Teplyakov, *J. Appl. Cryst.*, 1997, **30**, 1022.
34 A. W. Schüttelkopf, and D. M. F. van Aalten, *Acta Cryst.*, 2004, **D60**, 1355.
35 P. Emsley, and K. Cowtan, *Acta Cryst.*, 2004, **D60**, 2126.
36 A. T. Brünger, *Methods Enzymol.*, 1997, **277**, 366.
37 G. N. Murshudov, A. A. Vagin, and E. J. Dodson, *Acta Cryst.*, 1997, **D53**, 240.
38 I. W. Davis, A. Leaver-Fay, V. B. Chen, J. N. Block, G. J. Kapral, X. Wang, L. W. Murray, W. B. 3rd Arendall, J. Snoeyink, J. S. Richardson, and D. C. Richardson, *Nucleic Acids Res.*, 2007, **35**, W375.
39 W. L. DeLano, *The PyMOL Molecular Graphics System*, DeLano Scientific LLC: Palo Alto, CA, 2008; http://www.pymol.org/
40 M. J. Frisch, G. W. Trucks, H. B. Schlegel, G. E. Scuseria, M. A. Robb, J. R. Cheeseman, G. Scalmani, V. Barone, B. Mennucci, G. A. Petersson, H. Nakatsuji, M. Caricato, X. Li, H. P. Hratchian, A. F. Izmaylov, J. Bloino, G. Zheng, J. L. Sonnenberg, M. Hada, M. Ehara, K. Toyota, R. Fukuda, J. Hasegawa, M. Ishida, T. Nakajima, Y. Honda, O. Kitao, H. Nakai, T. Vreven, J. A. Montgomery, Jr., J. E. Peralta, F. Ogliaro, M. Bearpark, J. J. Heyd, E. Brothers, K. N. Kudin, V. N. Staroverov, R. Kobayashi, J. Normand, K. Raghavachari, A. Rendell, J. C. Burant, S. S. Iyengar, J. Tomasi, M. Cossi, N. Rega, J. M. Millam, M. Klene, J. E. Knox, J. B. Cross, V. Bakken, C. Adamo, J. Jaramillo, R. Gomperts, R. E. Stratmann, O. Yazyev, A. J. Austin, R. Cammi, C. Pomelli, J. W. Ochterski, R. L. Martin, K. Morokuma, V. G. Zakrzewski, G. A. Voth, P. Salvador, J. J. Dannenberg, S. Dapprich, A. D. Daniels, Ö. Farkas, J. B. Foresman, J. V. Ortiz, J. Cioslowski, and D. J. Fox, Gaussian, Inc., Wallingford CT, 2009.
41 D. A. Case, T. E. Cheatham, T. Darden, H. Gohlke, R. Luo, K. M. Merz, O. Onufriev, C. Simmerling, B. Wang, and R. J. Woods, *J. Comput. Chem.*, 2005, **26**, 1668.
42 J. Wang, W. Wang, P. A. Kollman, and D. A. Case, *J. Mol. Graphics Modell.*, 2006, **25**, 247.
43 M. H. M. Olsson, C. R. Søndergard, M. Rostkowski, and J. H. Jensen, *J. Chem. Theory Comput.*, 2011, **7**, 525.
44 D. A. Case, T. A. Darden, T. E. Cheatham III, C. L. Simmerling, J. Wang, R. E. Duke, R. Luo, R. C. Walker, W. Zhang, K. M. Merz, B. Roberts, S. Hayik, A. Roitberg, G. Seabra, J. Swails, A. W. Goetz, I. Kolossváry, K. F. Wong, F. Paesani, J. Vanicek, R. M. Wolf, J. Liu, X. Wu, S. R. Brozell, T. Steinbrecher, H. Gohlke, Q. Cai, X. Ye, J. Wang, M.-J. Hsieh, G. Cui, D. R. Roe, D. H. Mathews, M. G. Seetin, R. Salomon-Ferrer, C. Sagui, V. Babin, T. Luchko, S. Gusarov, A. Kovalenko, and P. A. Kollman, Amber Tools 13 and Amber 12, University of California, San Francisco, 2012.
45 W. L. Jorgensen, J. Chandrasekhar, and J. D. Madura, *J. Chem. Phys.*, 1983, **79**, 926.
46 J. Aqvist, *J. Phys. Chem.*, 1990, **94**, 8021.
47 T. A. Darden, D. York, and L. G. Pedersen, *J. Chem. Phys.*, 1993, **98**, 10089.
48 J.-P. Ryckaert, G. Ciccotti, and H. J. C. Berendsen, *J. Comput. Phys.*, 1977, **23**, 327.